Supporting information for:

Probing Radical-Molecule Interactions with a Second Generation Energy Decomposition Analysis of DFT Calculations Using Absolutely Localized Molecular Orbitals

Yuezhi Mao,*,† Daniel S. Levine,† Matthias Loipersberger,† Paul R. Horn,† and Martin Head-Gordon*,†,‡

† *Kenneth S. Pitzer Center for Theoretical Chemistry, Department of Chemistry, University of California at Berkeley, Berkeley, CA 94720, USA*

‡ *Chemical Sciences Division, Lawrence Berkeley National Laboratory, Berkeley, CA 94720, USA*

E-mail: yuezhi.mao@berkeley.edu; mhg@cchem.berkeley.edu

Table S1: Comparison of the total interaction energies and ALMO-EDA results (in kcal/mol) for the sandwiched benzene dimer radical cation and its neutral counterpart at varying intermolecular distances evaluated at the ωB97M-V/def2-QZVPPD level of theory.

			Radical Cation			
d(Å)	ELEC	PAULI	DISP	POL	CT	INT
2.7	-35.29	87.59	-20.95	-8.30	-26.49	-3.44
2.9	-21.16	49.04	-16.20	-6.09	-20.24	-14.66
3.1	-13.26	27.36	-12.42	-4.79	-15.50	-18.61
3.3	-8.82	15.21	-9.43	-3.92	-11.84	-18.79
3.5	-6.27	8.42	-7.13	-3.27	-8.96	-17.22
3.7	-4.77	4.64	-5.38	-2.76	-6.71	-14.98
3.9	-3.86	2.54	-4.03	-2.33	-4.96	-12.64
4.1	-3.27	1.38	-3.06	-1.97	-3.58	-10.51
4.5	-2.57	0.40	-1.84	-1.43	-1.74	-7.18
5.0	-2.06	0.08	-1.02	-1.00	-0.54	-4.54

			Neutral			
d(Å)	ELEC	PAULI	DISP	POL	CT	INT
2.7	-36.78	65.88	-23.11	-2.45	-3.53	36.80
2.9	-19.67	38.42	-18.06	-1.19	-1.93	17.23
3.1	-10.17	22.58	-14.01	-0.61	-1.10	6.85
3.3	-4.96	13.43	-10.78	-0.35	-0.65	1.65
3.5	-2.15	8.13	-8.25	-0.23	-0.39	-0.73
3.7	-0.68	5.05	-6.28	-0.16	-0.24	-1.63
3.9	0.07	3.24	-4.75	-0.12	-0.16	-1.78
4.1	0.42	2.17	-3.61	-0.09	-0.11	-1.64
4.5	0.60	1.12	-2.16	-0.05	-0.06	-1.15
5.0	0.51	0.62	-1.20	-0.03	-0.04	-0.64

Table S2: Comparison of the total interaction energies and ALMO-EDA results (in kcal/mol) for the T-shaped benzene dimer radical cation and its neutral counterpart at varying intermolecular distances evaluated at the ωB97M-V/def2-QZVPPD level of theory.

	Radical Cation					
d(Å)	ELEC	PAULI	DISP	POL	CT	INT
1.52	-21.30	54.19	-12.50	-8.10	-15.04	-2.76
1.72	-14.33	31.56	-9.77	-6.17	-10.43	-9.13
1.92	-10.04	18.06	-7.56	-4.84	-7.25	-11.63
2.12	-7.39	10.18	-5.80	-3.90	-5.07	-11.97
2.32	-5.72	5.67	-4.42	-3.19	-3.57	-11.24
2.52	-4.64	3.12	-3.34	-2.64	-2.56	-10.07
2.72	-3.91	1.70	-2.51	-2.20	-1.88	-8.81
2.92	-3.39	0.91	-1.90	-1.84	-1.42	-7.63
3.32	-2.67	0.26	-1.11	-1.29	-0.89	-5.71
3.82	-2.08	0.05	-0.61	-0.87	-0.58	-4.10

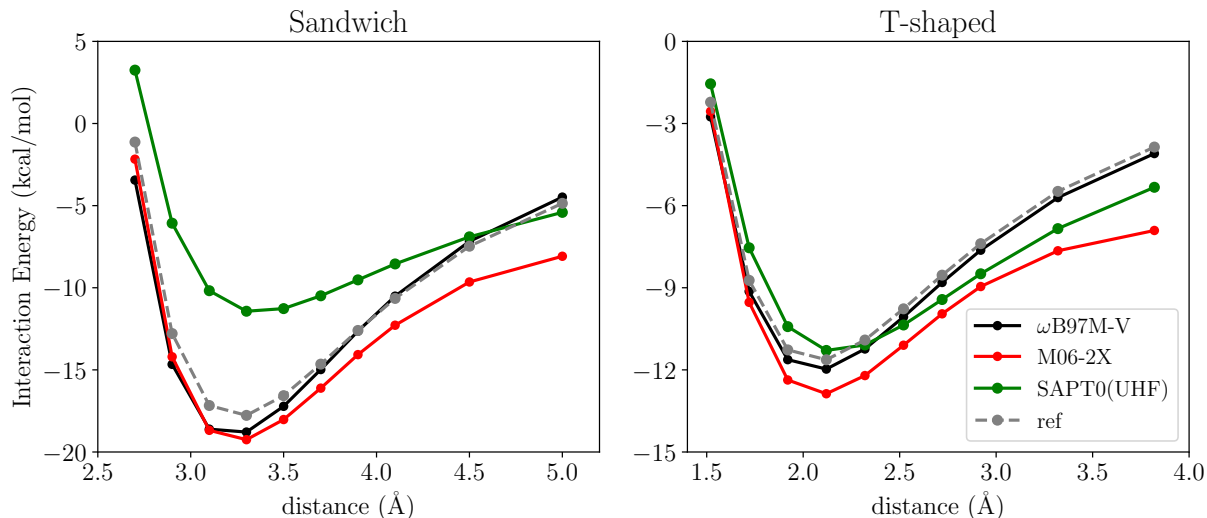|	Neutral					
d(Å)	ELEC	PAULI	DISP	POL	CT	INT
1.52	-20.99	59.43	-13.57	-3.27	-5.45	16.14
1.72	-12.68	34.93	-10.69	-1.92	-3.34	6.30
1.92	-7.62	20.19	-8.35	-1.13	-2.06	1.03
2.12	-4.59	11.49	-6.47	-0.69	-1.26	-1.52
2.32	-2.80	6.46	-4.97	-0.43	-0.78	-2.51
2.52	-1.75	3.59	-3.79	-0.28	-0.47	-2.71
2.72	-1.14	1.98	-2.88	-0.19	-0.29	-2.52
2.92	-0.77	1.08	-2.18	-0.13	-0.18	-2.19
3.32	-0.42	0.31	-1.29	-0.06	-0.08	-1.53
3.82	-0.24	0.06	-0.69	-0.03	-0.04	-0.94

Figure S1: Total interaction energies (in kcal/mol) of the sandwich (left panel) and T-shaped (right panel) benzene dimer radical cation at varying intermolecular distances calculated using ωB97M-V[S1] and M06-2X[S2] with the def2-QZVPPD[S3,S4] basis set. The SAPT0(UHF) results and the reference values are taken from ref. S5.

Table S3: Vertical ALMO-EDA results (in kcal/mol) for the sandwiched and T-shaped benzene dimer radical cations at minimum-energy distance and long range with different density functional approximations. Note that Grimme's -D3 correction with Becke-Johnson damping[S6] was applied to the calculations with BLYP[S7,S8] and B3LYP[S9] functionals.

| | Sandwiched (3.3 Å) | | | | Sandwiched (5.0 Å) | | | |
	ωB97M-V	M06-2X	BLYP	B3LYP	ωB97M-V	M06-2X	BLYP	B3LYP
ELEC	-8.82	-8.32	-8.22	-8.40	-2.06	-2.08	-1.84	-1.96
PAULI	15.21	13.85	14.16	14.25	0.08	0.06	0.07	0.08
DISP	-9.43	-8.28	-9.97	-9.79	-1.02	-0.44	-1.07	-1.06
POL	-3.92	-4.14	-3.40	-3.38	-1.00	-0.97	-0.95	-0.94
CT	-11.84	-12.36	-22.44	-18.84	-0.54	-4.66	-19.46	-13.79
INT	-18.79	-19.26	-29.88	-26.15	-4.54	-8.09	-23.26	-17.69
	T-shaped (2.12 Å)				T-shaped (3.82 Å)			
	ωB97M-V	M06-2X	BLYP	B3LYP	ωB97M-V	M06-2X	BLYP	B3LYP
ELEC	-7.39	-7.83	-6.93	-6.87	-2.08	-2.37	-1.95	-1.95
PAULI	10.18	8.96	9.51	9.73	0.05	0.04	0.04	0.04
DISP	-5.80	-4.73	-5.93	-6.01	-0.61	-0.31	-0.70	-0.69
POL	-3.90	-4.75	-4.12	-3.53	-0.87	-0.98	-0.92	-0.82
CT	-5.07	-4.52	-17.10	-13.47	-0.58	-3.28	-19.74	-13.69
INT	-11.97	-12.88	-24.57	-20.15	-4.10	-6.91	-23.26	-17.11

Table S4: Adiabatic ALMO-EDA results for the Bz$^{+\bullet}$−Py and Naph$^{+\bullet}$−Py complexes. ΔE_{bind} describes the energy lowering relative to the individually relaxed fragments at each intermediate state, $r(\text{C}-\text{N})$ stands for the distance between the N atom of pyridine and the C atom on the aromatic ring attacked by it, and the bending of the C−H bond is described by the $\text{C}_1-\text{C}_2-\text{C}_3-\text{H}_1$ dihedral, where C1 is the attacked C atom, C2 and C3 are the two adjacent C atoms on the aromatic ring, and H1 is the hydrogen atom attached to C1. A negative dihedral angle corresponds to bending away from the attacking direction.

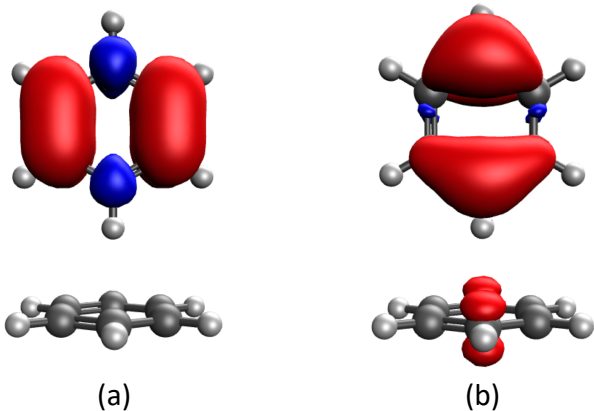|	Bz$^{+\bullet}$−Py			Naph$^{+\bullet}$−Py		
	FRZ	POL	FULL	FRZ	POL	FULL
ΔE_{bind} (kcal/mol)	-8.11	-11.95	-40.48	-7.91	-10.91	-24.78
$r(\text{C}-\text{N})$ (Å)	3.10	2.84	1.53	3.66	3.48	1.53
C−H bending angle (°)	0.0	-0.1	-28.8	0.0	0.0	-28.6

(a)   (b)

Figure S2: Spin density plots (isovalue = 0.002 a.u.) for the full SCF solutions of the T-shaped benzene dimer radical cation: (a) the unstable solution, which is obtained when one uses concatenated isolated fragment orbitals as the initial guess; (b) the stable SCF solution.

Table S5: Vertical ALMO-EDA results (in kcal/mol) for the $^{\bullet}$OH(H$_2$O) complex in the $^2A'$ and $^2A''$ both at the global equilibrium geometry (optimized in $^2A'$).

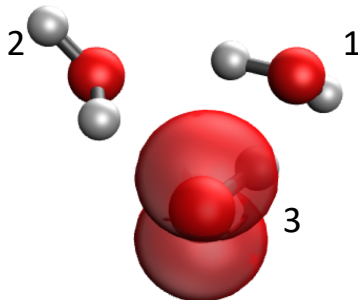|	ELEC	PAULI	DISP	POL	CT	INT
$^2A'$	-9.39	8.78	-1.80	-1.50	-2.00	-5.91
$^2A''$	-9.14	8.84	-1.80	-1.49	-1.98	-5.56

Figure S3: Spin density plot (isovalue = 0.005 a.u.) for the stable structure of $^\bullet$OH(H$_2$O)$_2$ calculated at the ωB97M-V/def2-TZVPD level of theory.

Table S6: Frozen energy decomposition results (in kcal/mol) for the MBE of the $^\bullet$OH(H$_2$O)$_2$ complex and the H$_2$O trimer.

| | $^\bullet$OH(H$_2$O)$_2$ | | | | |
	ΔE_{12}	ΔE_{13}	ΔE_{23}	ΔE_{3b}	ΔE_{123}
ELEC	-9.43	-11.17	-6.87	0.00	-27.48
PAULI	9.96	12.46	7.23	-0.18	29.47
DISP	-2.14	-2.21	-1.75	0.15	-5.95
	H$_2$O trimer				
	ΔE_{12}	ΔE_{13}	ΔE_{23}	ΔE_{3b}	ΔE_{123}
ELEC	-9.75	-8.80	-9.71	0.00	-28.25
PAULI	10.43	9.52	10.38	-0.23	30.10
DISP	-2.17	-2.09	-2.17	0.15	-6.28

Table S7: Energies of the A' and A'' states for the pre-reactive complexes for by $^\bullet$OH with HCHO/CH$_3$CHO (in Hartree) and the differences (in kcal/mol) between them ($\Delta E = E(A'') - E(A')$). The ωB97M-V and M06-2X results are calculated using re-optimized geometries within each individual electronic state (A' or A''), while the MP2 results are calculated using geometries directly taken from ref. S10.

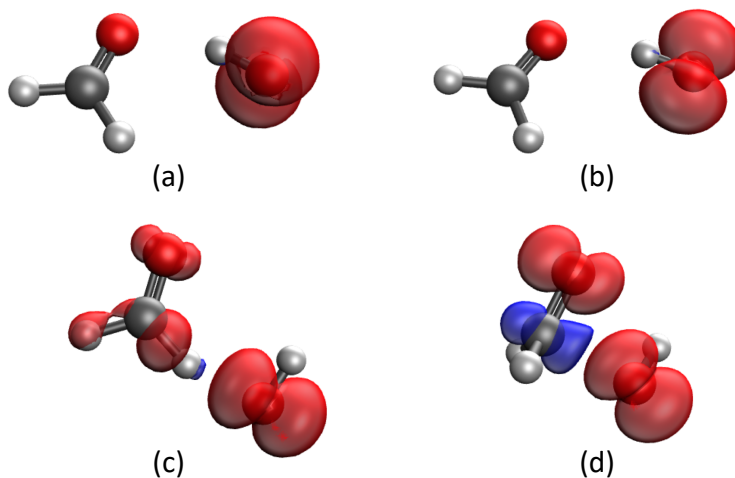|		$E(A')$	$E(A'')$	ΔE
	ωB97M-V	-190.259278	-190.259914	-0.40
HCHO	M06-2X	-190.242283	-190.242821	-0.34
	MP2	-189.829188	-189.829790	-0.38
	ωB97M-V	-229.579334	-229.579937	-0.38
CH$_3$CHO	M06-2X	-229.564966	-229.565466	-0.31
	MP2	-229.038415	-229.039009	-0.37

Figure S4: Spin density plots (isovalue = 0.005 a.u.) for the stationary structures along the •OH + HCHO reaction path at the full SCF solution: (a) the A'' state for the •OH$\cdots$OCH$_2$ pre-reactive complex (PRC(F)); (b) the A' state for PRC(F), whose energy is 0.4 kcal/mol higher than that of A''; (c) the transition state for H-abstraction (TS1(F)); (d) the transition state for nucleophilic addition to the carbonyl group (TS2(F)).

Table S8: Full ALMO-EDA results (in kcal/mol) for the characterized PRC and TS structures in the •OH + HCHO and •OH + CH$_3$CHO reactions. The calculations are performed at the ωB97M-V/def2-TZVPD level of theory.

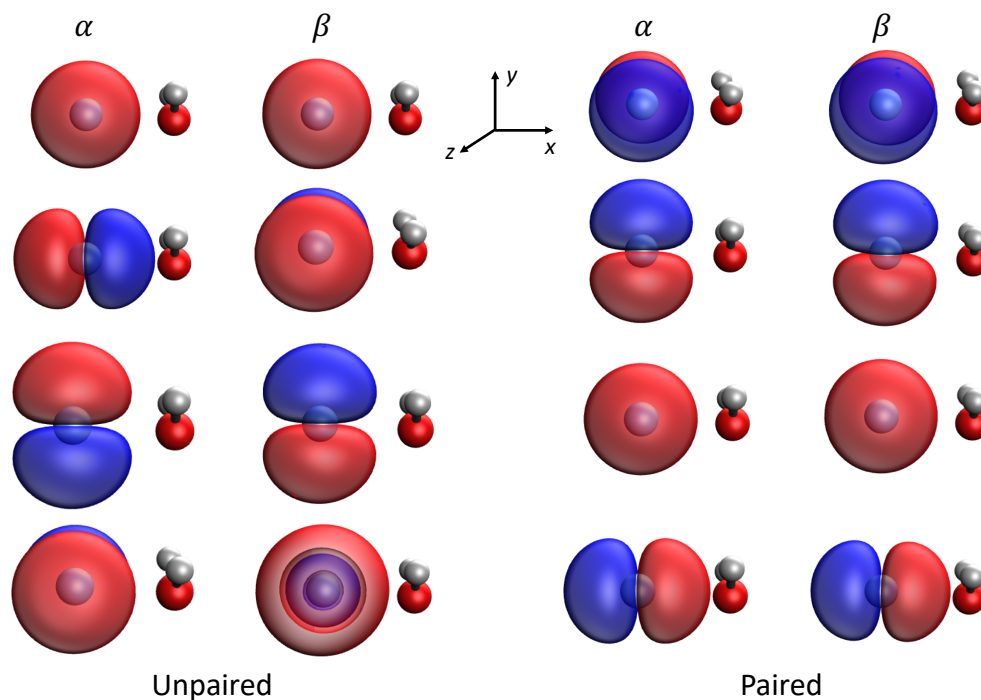|	ELEC	PAULI	DISP	POL	CT	INT
PRC(F)	-9.01	9.22	-2.21	-1.57	-2.03	-5.59
TS1(F)	-9.06	23.72	-3.23	-2.01	-11.26	-1.85
TS2(F)	-26.65	63.02	-6.65	-5.55	-25.76	-1.60
PRC(A)	-10.39	10.55	-2.35	-1.89	-2.42	-6.50
TS1(A)	-9.60	23.52	-3.54	-2.01	-10.97	-2.59

Figure S5: Illustration of the Löwdin orbital pairing[S11] scheme employed in the calculation of the rehybridization (REHYB) energy. From top to bottom are the 2nd to 5th orbitals of α or β spin on the F$^\bullet$ fragment. The left panels show the original, unpaired orbitals that are directly obtained from a fragment USCF calculation, among which the α orbitals (from top to bottom) are of $2s$, $2p_x$, $2p_y$, and $2p_z$ characters and the β orbitals $2s$, $2p_z$, $2p_y$, and $3s$. The right panels show the transformed orbitals according to Löwdin's orbital pairing scheme, and each corresponding pair of α and β orbitals is of the same character ($2p_z$, $2p_y$, $2s$, and $2p_x$ from top to bottom). The orbitals are generated from M06-2X[S2]/def2-TZVPD[S3,S4] calculations and are visualized with an isovalue of 0.02 a.u. except for the substantially more diffuse $3s$-like orbital, for which a higher isovalue 0.04 a.u. is used.

References

(S1) Mardirossian, N.; Head-Gordon, M. ωB97M-V: A combinatorially optimized, range-separated hybrid, meta-GGA density functional with VV10 nonlocal correlation. *J. Chem. Phys.* **2016**, *144*, 214110.

(S2) Zhao, Y.; Truhlar, D. G. The M06 suite of density functionals for main group thermochemistry, thermochemical kinetics, noncovalent interactions, excited states, and transition elements: two new functionals and systematic testing of four M06-class functionals and 12 other functionals. *Theor. Chem. Acc.* **2008**, *120*, 215–241.

(S3) Weigend, F.; Ahlrichs, R. Balanced basis sets of split valence, triple zeta valence and quadruple zeta valence quality for H to Rn: Design and assessment of accuracy. *Phys. Chem. Chem. Phys.* **2005**, *7*, 3297–3305.

(S4) Rappoport, D.; Furche, F. Property-optimized Gaussian basis sets for molecular response calculations. *J. Chem. Phys.* **2010**, *133*, 134105.

(S5) Gonthier, J. F.; Sherrill, C. D. Density-fitted open-shell symmetry-adapted perturbation theory and application to π-stacking in benzene dimer cation and ionized DNA base pair steps. *J .Chem. Phys.* **2016**, *145*, 134106.

(S6) Grimme, S.; Ehrlich, S.; Goerigk, L. Effect of the damping function in dispersion corrected density functional theory. *J. Comput. Chem.* **2011**, *32*, 1456–1465.

(S7) Becke, A. D. Density-functional exchange-energy approximation with correct asymptotic behavior. *Phys. Rev. A* **1988**, *38*, 3098.

(S8) Lee, C.; Yang, W.; Parr, R. G. Development of the Colle-Salvetti correlation-energy formula into a functional of the electron density. *Phys. Rev. B* **1988**, *37*, 785.

(S9) Becke, A. D. Density-functional thermochemistry. III. The role of exact exchange. *J. Chem. Phys.* **1993**, *98*, 5648–5652.

(S10) Alvarez-Idaboy, J. R.; Mora-Diez, N.; Boyd, R. J.; Vivier-Bunge, A. On the importance of prereactive complexes in molecule-radical reactions: hydrogen abstraction from aldehydes by OH. *J. Am. Chem. Soc.* **2001**, *123*, 2018–2024.

(S11) Löwdin, P.-O. On the non-orthogonality problem connected with the use of atomic wave functions in the theory of molecules and crystals. *J. Chem. Phys.* **1950**, *18*, 365–375.